

Distribution and Flow Control In Different Aspect Ratio Manifolds with High Speed Flow

N. Findanis¹

¹Department of Engineering
Pentair, New South Wales 2214, Australia

Abstract

In almost all applications of industrial pipe flows, there is the requirement to distribute the flow of fluid. The flow distribution can be achieved by the manifold flow device. However, there is a deficiency of studies in the area of flow distribution in manifolds with high speed flows. The present work is aimed at providing a further understanding of high speed flow distribution in manifolds and improving the flow efficiency in manifolds. The key parameter that is investigated is the aspect ratio of manifolds. The flow field is controlled or influenced by using passive flow control methods to incline the fluid flow into flow paths, directing them into the desired branches of flow connections. The different manifold configurations were analysed computationally. A comparison was initially focused between the reference base configuration flow field through the different aspect ratio manifolds. The velocity field and the eddy viscosity parameters were compared between the simulated flow models to ascertain the key features in the distributed flow field and especially, to determine the areas that showed greater flow recirculation or flow eddies and the separated flow regions. Each aspect ratio manifold model was then modeled with the range of passive flow control devices and compared to the unmodified base model which acted as the reference simulation. The CFD study was conducted as a high speed flow/compressible flow regime accounting for the ideal gas dynamic model being air as the working fluid. The study showed that the flow field can be significantly altered depending on the passive flow control device employed and that efficiency gains can be achieved in high speed flows that can be of benefit to the above mentioned industrial and other engineered flow applications.

Introduction

The transport of fluids is critical and necessary in many industrial and commercial applications in various activities and tasks that are performed around the world for the continual function and advancement of mankind [1]. It is common that a fluid when it is transported or used for a process as a working fluid or purely to be transported to be used in an application that it will be required to distribute the fluid apportioned in a network of piping branches [2]. The fluid regime for transport of fluids is frequently in the turbulent flow regime of subsonic flows. However, an important area for fluid mechanics is the transport of fluid at high speed or high speed flows in high velocity pipelines, reverse pulse-jet

cleaning systems, compressor pipeline flows etc. in industrial plants [3]. In this particular paper the focus is on high speed flows in the transport of fluids for different process that occur in aspects of industrial flow applications that require the distribution of fluids through manifolds.

There is a deficiency in the available literature for the examination of how the efficiency in manifolds can be improved for high speed flow networks. The examination of losses in a pipe [3] network and in particular for this paper, manifolds, can substantially contribute to the improvement of the dynamics of flow through the system to lower the power requirement of compressors and pump to push the fluid through the system. The manifold can contribute a substantial amount of the losses in the network [4, 5, 6]. Typically in piping network systems there is a need to consider the entry and exit losses, sudden or gradual expansion/contraction, bends and branches and direction change of flow. These flow loss elements can be all contained in a single manifold unit in system that could consist many manifolds making for a large percentage of the total losses in the system. Another, source that contributes to the flow losses in a manifold is the ability to efficiently distribute and turn the flow for each branch, inlet/s to outlet/s on the manifold.

This paper examines the use of passive flow control devices that could be used in manifolds to improve the efficiency of the flow through this ubiquitous flow distribution element when used for high speeds flow regimes in industrial pipe flow applications.

Computational Methodology

The computational analysis was conducted in a three-dimensional space domain. The symmetrical half-solid models were constructed and used in the CFD analysis as the fluid volume shown below in Figures 1 through to Figure 4.

Shown in Figure 1 is the base or reference case geometry of one particular configuration of manifold used in the CFD analysis. The reference case was used as the baseline with which to compare the cases that used a passive flow control (PFC) device. There were three passive flow control devices used, PFC1, PFC2 and PFC3.

The flow distribution in the manifolds was applied at three different aspect ratios of 0.25 ($\frac{1}{4}$), 0.125 ($\frac{1}{8}$) and 0.0625 ($\frac{1}{16}$). The aspect ratios (AR) were calculated using the equation (1),

$$AR = \frac{D_o}{L} \quad - (1)$$

Where,

D_o – is the diameter of the manifold

L – is the length of the manifold

There were two different manifold diameters that were used. The manifold diameter of 100 mm and the equivalent manifold diameter at 50% of the area of that at 100 mm, which results in a diameter of 70.71 mm [7]. There were four branch outlets on either side of the manifold, symmetrically opposed. The diameter of the branch outlets were 25 mm for the manifold with 100 m diameter and likewise area scaled by 50% to 17.68 mm for the 50% area manifold. The spacing between the branches was equidistance on the centrelines according to the length of the manifold as determined from the AR.

The three passive flow control devices are shown I figures 2 through to 4. PFC1 consists of dimples that have been located on the centreline of the branches of each outlet. The dimples are of 10 mm diameter of hemi-spherical shape for the 100 mm diameter manifold. As previously, the dimples are area scaled down for the 50% area manifold.

PFC2 also uses dimples as a means to control the flow and improve distribution in the manifold. The dimples in this configuration are placed before the flow is incumbent on the branch in the manifold. Instead of using single dimple, the dimples are evenly distributed around the circumference of the cylindrical manifold. Additionally, there is not a single row of dimples that is used but rather there are three rows in total equally spaced. The dimples are 5 mm in diameter for the 100 mm diameter manifold and are scaled down to 50% area, as previously, for the 50% area manifold.

In the PFC3, a different passive flow control concept is utilised. In this approach, volume is subtracted from the manifold by using pod that is located down the centreline of manifold. The pod or rod insert is not a plain cylindrical but also incorporates geometry using bulb type protrusion located fore of the branches on the manifold. The bulbs are designed to encourage the flow into the branches of the manifold.

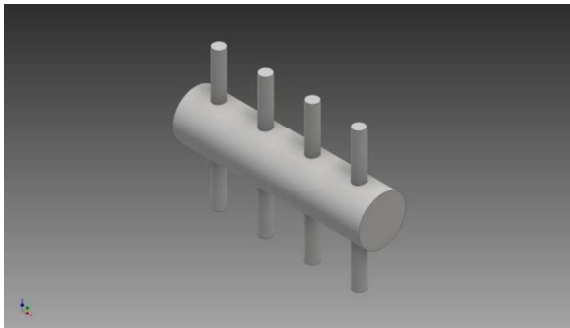


Figure 1. Ref., 0.25 Aspect Ratio, $\varnothing 100$ mm.

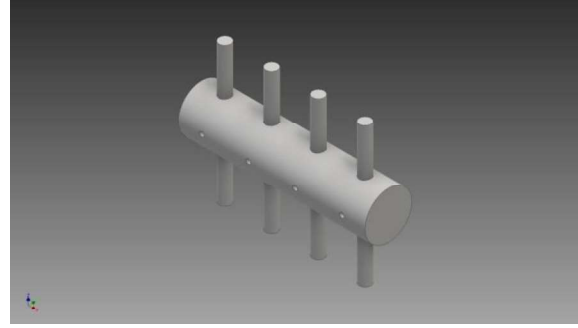


Figure 2. PFC1, 0.25 Aspect Ratio, $\varnothing 100$ mm.

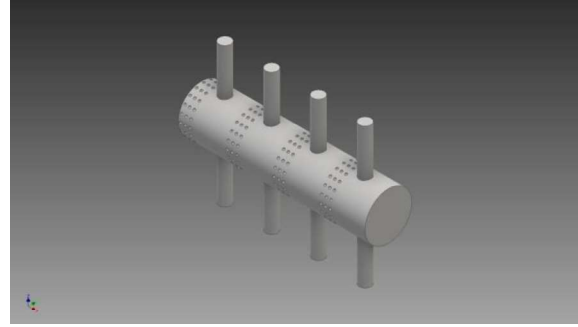


Figure 3. PFC2, 0.25 Aspect Ratio, $\varnothing 100$ mm.

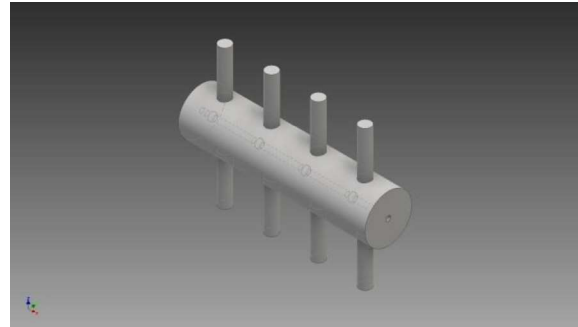


Figure 4. PFC3, 0.25 Aspect Ratio, $\varnothing 100$ mm.

The boundary conditions were constrained in the physics setup of the simulation. As mentioned, the fluid domain was constructed as a half-model symmetrical on the longitudinal centre plane. To generate the high speed flow through the manifold an inlet condition was defined as a total pressure of 600 kPa. The outlets were at atmospheric pressure, relative static of zero, on each of the branches on the manifold. See Figure 5.

The three-dimensional governing equations for the flow of an incompressible fluid are solved namely the unsteady Reynolds Averaged Navier-Stokes equations. The conservation of mass and momentum equations are shown as equations (2) and (3).

$$(2) \nabla \cdot \bar{\mathbf{u}} = 0$$

$$(3) \rho \frac{\partial \bar{\mathbf{u}}}{\partial t} + \rho \bar{\mathbf{u}} \cdot \nabla \bar{\mathbf{u}} = -\nabla \bar{p} + (\mu + \mu_t) \nabla^2 \bar{\mathbf{u}}$$

The simulation is conducted as a steady state analysis for all cases with and without flow control device applied. High resolution turbulence numerics based on the advection and transient scheme is used in the turbulence modelling [4]. The turbulence model used to

calculate the averaged turbulent stresses is based on Menter Shear Stress Transport (SST) two-equation model [4] being the most suitable when flow separation occurs in the flow field.

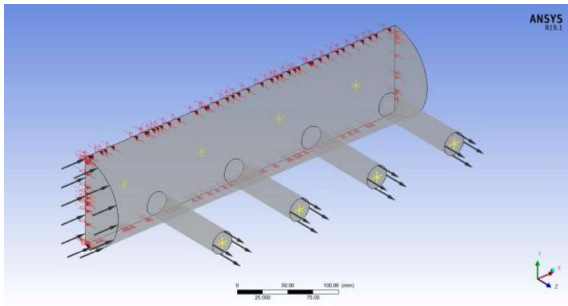
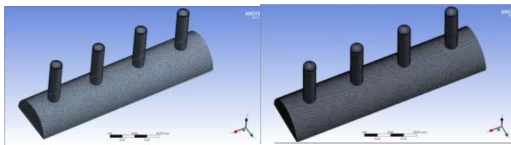


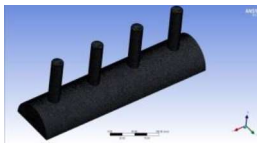
Figure 5. CFD Boundary Conditions.

A grid independent study was conducted to ensure an accurate solution to the CFD analysis. This was conducted using the three different mesh densities. The results show that a minimum deviation occurred between the medium and fine grid densities. Thus, it was decided that to maintain the integrity of the solution that only the medium mesh was required in the present work. The meshes are shown in Figure 6.



a) Coarse

b) Medium



c) Fine

Figure 6. Meshes. a) coarse, b), medium, c) fine.

Results and Discussion

The eddy viscosity contour results of the numerical CFD analysis are given in Figures 7 through to Figure 11. The inlet side of the manifold for each case is on the right side of manifold contour plots. The eddy viscosity is able to show more clearly the turbulent transfer of energy or the eddies that are created by the passive flow control devices that can result in flow directional changes to improve the flow distribution. Branch outlets are numbered 1 through 4, from right to left (+x axis).

The results for high speed pipe flow [3] were used to provide an approximate reference validation for the current manifold study.

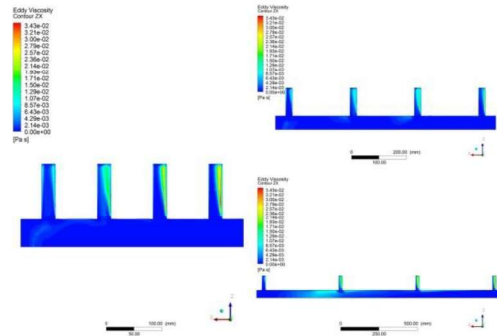


Figure 7. Ref. Cases. Clockwise from left AR (0.25, 0.125 & 0.0625), \varnothing 100 mm manifold. Eddy Viscosity.

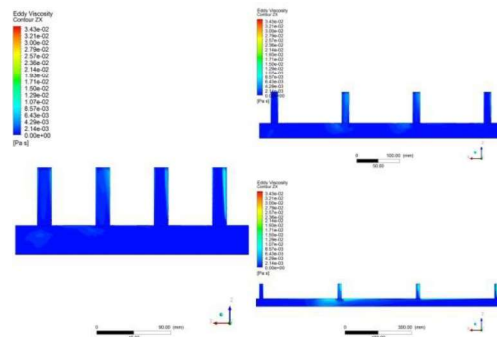


Figure 8. Ref. Cases. Clockwise from left AR (0.25, 0.125 & 0.0625), \varnothing 70.71 mm manifold. Eddy Viscosity.

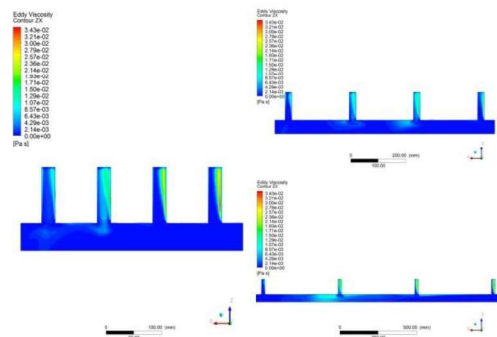


Figure 9. PFC1 Cases. Clockwise from left AR (0.25, 0.125 & 0.0625), \varnothing 100 mm manifold. Eddy Viscosity.

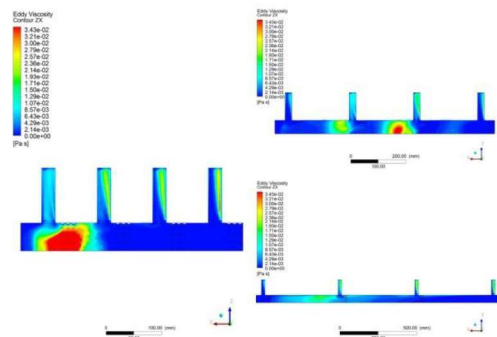


Figure 10. PFC2 Cases. Clockwise from left AR (0.25, 0.125 & 0.0625), \varnothing 100 mm manifold. Eddy Viscosity.

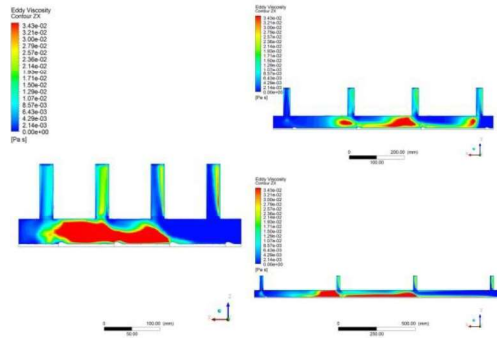


Figure 11. PFC3 Cases. Clockwise from left AR (0.25, 0.125 & 0.0625), $\varnothing 100$ mm manifold. Eddy Viscosity.

The reference cases show that the smaller diameter has a better flow distribution as shown between figures 7 and 8, with a decrease in the eddy viscosity for the $\varnothing 70.71$ mm manifold. However, at 50% area, the mass flow rate is approximately half for each AR and each PFC device.

The mass flow rate change between the reference cases and those with the use of the PFC devices was not substantial. The maximum change of 1.15% was for the case that uses PFC3. This was expected as it reduces the internal volume of the manifold much more than the other PFC's.

The use of PFC's on the larger AR manifold (0.25) does not contribute to the improvement of the flow distribution through the manifold. Rather, using a PFC device reduces the mass flow rate, depending on the PFC used, and creates an unnecessary increase in the eddy viscosity.

The high pressure inlet is very close to the first outlet branch on the manifold. This close proximity to undeveloped flow prevents the PFC device from being able to have an effect on the flow and provide any improvements to the flow distribution. Additionally the final outlet branch which is closest to the end of manifold has the highest static pressure resulting in a uniform flow out of this branch and thus not requiring the use of a PFC device in this location, with these types of manifold configuration having a blocked end face.

The PFC device PFCs, as shown in figure 9, has only a minimal effect in aiding the flow distribution for the 0.125 and 0.0625 AR manifolds for branch outlets 2 and 3. As a single dimple that is placed on the centreline of each of the branches, it can only assist the flow in this small way considering the diameter of the hemi-sphere is small too. There is a very slight mass flow increase for 50% manifold diameter for AR 0.25 and 0.125.

With PFC3, as shown in figure 11, it results in the highest generation of the turbulence energy for all AR's, and is significantly large for the high AR of 0.25, the shortest manifold. It can be seen in figure 11, that it can affect the flow towards the entry side of the manifold due to its flow intrusive geometry. PFC3 is effective in introducing turbulence for AR 0.125 and 0.0625, however non-effective in this case, towards the end face

of the manifold, on the last outlet branch, branch 4, where the static pressure is highest. The geometry of the bulb on the PFC device only slightly contributes to improving the flow distribution in the branches of the manifold across the outlet. Especially considering that the mass flow rate is more substantially affected than the other PFC's. Surprisingly, there is a mass flow rate increase for an AR of 0.125 of 0.15% and 0.22% for the 100 mm and 70.71 mm manifold diameter, respectively.

Using PFC2 as shown in figure 10, it produces a more uniform flow through the branch outlets, especially branches 2 & 3 for AR 0.125 and 0.0625.

Conclusions

The simulation study showed that the flow field can be significantly altered using PFC2 & PFC3 for the lower AR manifolds. There were configurations in which the manifold resulted in an increase in the mass flow rate whilst concomitantly improving the flow distribution. It was found that PFC2 improved most the uniformity of the flow distribution in the manifold branch outlets. Future research will be to perform experimental validation of the simulation results on high speed flow manifolds, as there are a lack of available experimental results in this field. Further, it would be required to investigate transient high speed flows, as this is commonly the scenario in this flow regime. Also, other more innovative flow control is required to achieve significant flow improvements.

Acknowledgments

I would like to acknowledge the generous use of the computer facilities made available.

References

- [1] Cengel, Y.A., Cimbala, J.M., Fluid Mechanics, 2nd Edition, Mc Graw Hill, 2006.
- [2] Wang, J., Theory of Flow Distribution in Manifolds, *Journal of Chemical Engineering*, Vol. 168, Iss. 3, 2011, 1331-1345.
- [3] Findanis, N., Internal Flow: Pipe Losses Steady State and Transient Analysis, 20th AFMC, 2016.
- [4] Pigford, R.L., Ashraf, M., Miron, Y.D., Flow Distribution in Piping Manifolds, *Journal of Industrial & Engineering Chemistry Fundamentals*, Vol. 22, Iss. 4, 1983, 463-471.
- [5] Hassan, J.M., Mohamed, T.A., Mohamed, W.S., Wissam, H.A., Modeling the Uniformity of Manifold With Various Configurations, *Journal of Fluids*, Vol. 2014, 2014.
- [6] Bajura, R.A., Jones Jr. E.H., Flow Distribution Manifolds, *Journal of Fluids Engineering, Transactions of the ASME*, Vol. 98, No. 4, 654-666, 1976.
- [7] Choi, S.H., Shin, S., Cho, Y.I., The Effect of Area Ratio on the Flow Distribution in Liquid Cooling Module Manifolds for Electronic Packaging, *International Communications in Heat and Mass Transfer*, Vol. 20, No. 2, 221-234, 1993.
- [8] Menter FR. Zonal two equation k- ω turbulence models for aerodynamic flows. AIAA paper 93-2906.